Dalton Transactions

Influence of magnetic dilution on relaxation processes in a solid solution comprising tetrahedral Co/Zn^{II} complexes

Journal:	*Dalton Transactions*
Manuscript ID	DT-ART-03-2020-001058
Article Type:	Paper
Date Submitted by the Author:	20-Mar-2020
Complete List of Authors:	Ceglarska, Magdalena; Uniwersytet Jagiellonski w Krakowie Wydzial Fizyki Astronomii i Informatyki Stosowanej, Department of Advanced Materials Engineering Stefańczyk, Olaf; The University of Tokyo, School of Science, Department of Chemistry Ohkoshi, Shin-ichi; The University of Tokyo, Department of Chemistry, School of Science Majcher-Fitas, Anna; Uniwersytet Jagiellonski w Krakowie Wydzial Fizyki Astronomii i Informatyki Stosowanej, Department of Advanced Materials Engineering

Journal Name

ARTICLE TYPE

Cite this: DOI: 00.0000/xxxxxxxxxx

Influence of magnetic dilution on relaxation processes in a solid solution comprising tetrahedral Co/Zn^{II} complexes†

Magdalena Ceglarska,[a] Olaf Stefańczyk,[b] Shin-ichi Ohkoshi,[b] and Anna M. Majcher-Fitas*[a]

Received Date
Accepted Date

DOI: 00.0000/xxxxxxxxxx

Single Ion Magnets have long been considered good prospective candidates to record a bit of information. One of the smallest known Single Ion Magnets is $CoBr_2(pyridine)_2$. This molecular compound exhibits slow relaxation of magnetization mainly due to the thermally activated Orbach process, [Majcher *et al.*, *Chem. Sci.*, 2018, **9**, 7277–7286.] however, the total relaxation time is dramatically shortened at low temperatures due to the direct, Raman, and quantum tunneling of magnetization processes. At low temperatures, the distribution of the probability of the possible relaxation pathways in this case favour QTM and the direct process over the Orbach process. To elongate the relaxation time, the compound was diluted with diamagnetic Zn^{II}, producing 5 analogues of the general formula: $Co_xZn_{1-x}Br_2(pyridine)_2$ (x = 0.91, 0.67, 0.43, 0.24, 0.06), confirmed to be a solid solution by independent experimental techniques (powder X-Ray diffraction, infrared spectroscopy). The presence of diamagnetic Zn^{II} ions change the distribution of the dipolar interactions between the Co^{II} centres in the material, which results in a monotonous change in the relaxation times, which become longer with increasing dilution, which is explained by diminishing QTM contribution. The appearance of multiple relaxation processes is also observed for higher x, which is explained as the creation of multiple, separate frequency domains, as a result of the competition between QTM and the direct process contributions. We present a thorough, systematic study of magnetic dilution, which will hopefully be useful to estimate optimal dilutions in similar solid solutions.

1 Introduction

Molecular magnets are a relatively young group of magnetic materials with many great potential applications.[1] The magnetism in such materials originates from unpaired electrons of *d* or *f* orbitals of paramagnetic metal ions, or organic radicals. These magnetic centers are parts of building blocks, which can form structures of different dimensionality. Low-dimensional molecular magnets (0D and 1D) deserve special attention due to the slow relaxation of magnetization phenomenon they display.[2] This feature enables treating them as prospective materials for high density data storage or the new field of molecular spintronics.[3] The best candidates are the smallest ones - Single Ion Magnets (SIMs), comprising only one magnetic centre in a single molecule.[4] The size of the molecular units depends mostly on the size of the ligands and their spatial arrangement.

Recently, most of the research in this area is devoted to obtaining Single Ion Magnets with high blocking temperatures (preferably above 77 K) and long relaxation times.[5] The key is strong spin–orbit coupling and large unquenched angular momentum, which both contribute to the high uniaxial anisotropy.[6,7] The perfect candidates for that are lanthanides and many compounds based on them have been thoroughly investigated in recent years.[8,9,10] Due to these investigations, several basic rules were found that govern the magnetic properties of Single Ion Magnets. They are a significant help on the level of designing of discreet complexes with large energy barrier, among which, those based on Dy^{III} achieve the highest values.[11,12] However, what influences the contributions of specific relaxation processes to the total relaxation time is still being elucidated. In lathanide-based SIMs, the energy level scheme is quite complicated and often clouds the general analysis. We propose a different approach – a detailed analysis of a Co^{II}-based Single Ion Magnet solid solution where the energetic diagram is more simple and the path-

[a] *Faculty of Physics, Astronomy and Applied Computer Science, Jagiellonian University, Łojasiewicza 11, 30-348 Krakow, Poland.*
[b] *Department of Chemistry, School of Science, The University of Tokyo, 7-3-1 Hongo, Bunkyo-ku, Tokyo 113-0033, Japan.*

† Electronic Supplementary Information (ESI) available: [details of any supplementary information available should be included here]. See DOI: 00.0000/00000000.

ways of different relaxation processes are more clear. Due to the values of energy barriers being significantly lower in comparison to compounds with lanthanides,[11] the Co^{II} compounds noted a slight decrease in interest lately. However, a thorough analysis of a Co^{II}-based SIM will be a stepping stone providing a starting model on how the relaxation processes change with dilution and may be helpful for analysing more complicated systems.

Co^{II} ions exhibit strong magnetic anisotropy which is the main reason why the so-called energy barrier of a relaxation process is observed.[13] Another very important factor is the presence of spatially extended ligands which prevent magnetic interaction between molecules.[14] In SIMs, it is extremely important at the level of designing to properly choose the building blocks. One of the smallest known Co^{II}-based single ion magnets is $CoBr_2(pyridine)_2$.[15] In this case, the ligands are not very extended but are appropriately arranged in the structure - distorted tetrahedron. Apart from that, the orbitals of Br do not prefer to connect to two Co^{II} simultaneously. Also, no hydrogen bonds were detected in the structure. Therefore, there is no possible way to transfer exchange interaction between magnetic centers. Moreover, the dipolar interactions are too weak to cause magnetic ordering. For this compound, the magnetic relaxation process is not visible without a DC magnetic field, because the relaxation times are too short to be measured using available methods. At a sufficiently high DC magnetic field, the relaxation times are long enough to be measured using AC susceptometry. The field value of 2.5 kOe was chosen as optimal. The observed effective energy barrier U_{eff}/k_B determined using only the Arrhenius law to analyse the relaxation times is equal to 28(2) K. Obtaining a cross-linked polymeric matrix of this compound by using poly(4-vinylpyridine) with pyridine rings forming the crystalline SIM caused the relaxation times to become longer. Such behaviour is characteristic for some solid solutions of molecular magnets[16] but in this case, the obtained material did not have a crystal structure. This observation prompted the research presented herein - we decided to explore the likely solid solution behaviour of this crystalline compound and the influence of diluting it with diamagnetic species on the contribution of individual relaxation mechanisms. A summary of these mechanisms might be useful to the Reader and is presented below.

For Co^{II} in a tetrahedral complex, the energy levels are split into doublets according to the Kramers theory by zero-field splitting (ZFS).[17] Between the molecules in a SIM material, there are no exchange interactions, that is why the system can be describerd by the following Hamiltonian:

$$\mathscr{H}_{CF} = D[S_z^2 - \frac{1}{3}S(S+1)] + E(S_x^2 - S_y^2) + \mu_B g \mathbf{S}\cdot\mathbf{H}, \qquad (1)$$

where D is the axial magnetic anisotropy parameter and E is the second-order rhombic anisotropy parameter.[18] The energy gap between the $\pm 3/2$ and $\pm 1/2$ states can be estimated from the equation:

$$\delta = 2\sqrt{D^2 + 3E^2} \qquad (2)$$

The arranegement of spin levels is specified by the sign of the D parameter. For positive D, the states with the lowest $|M_s|$ have the lowest energy, and for negative D the states with the highest $|M_s|$ have the lowest energy.

In tetrahedral complexes of Co^{II} $|D|$ takes values from a very wide range - from around 2 cm^{-1} [19] up to even 160 cm^{-1}.[20–22] Currently, chemical modifcations of structures are introduced to obtain higher values of the D and E parameters, and therefore, a higher energy barrier.[23]

However, even if the energy barrier value is very high, it does not imply a long relaxation time. This is due to the presence of very fast quantum tunneling of magnetization (QTM).[24] A very significant role in this process is played by the dipolar interactions and collective nuclear magnetic field.[25,26] To weaken them both, magnetic dilution is used, causing the relaxation times to become longer as a result of the supression of QTM. In the case of dilution with diamagnetic ions, the dipolar interactions are counteracted, however, the nuclear field comes not only from the metal centers but also from the ligands, therefore, dilution does not affect this aspect significantly. The other method to elongate the relaxation times is to apply an external DC magnetic field of moderate value. Both of these methods enable splitting the lowest lying Kramers doublet enough to make QTM much less probable.

Magnetic dilution has been applied to many SIMs to elongate the relaxation times in low temperature[21,27–30] and also proved to be an effective tool to investigate the multiple-relaxation processes.[31?] Especially interesting for us is the case of Co^{II} seven-coordinate complex: $[Co(DAPBH)(NO_3)(H_2O)](NO_3)$.[31] This complex was magnetically diluted with Zn^{II} analogue (Co^{II} concentrations: 25, 10 and 5%). There are two relaxation processes present in non-zero DC magnetic field and on the basis of the ratio between χ'' maximal values of both processes for undiluted and diluted compounds, one of the process was determined as of intramolecular origin, while the second - intermolecular origin. This compound is also an example of SIMs with large positive anisotropy (D = 30 cm^{-1}), which was long considered as an obstacle in obtaining SIMs/SMMs with high relaxation energy barrier.[18]

The temperature and field dependence of relaxation time which takes into consideration all of the four possible pathways of relaxation processes for single spins is (Orbach, Raman, direct and QTM, respectively)[29,32]:

$$\tau_{SIM}^{-1} = \tau_0^{-1} exp(-U_{eff}/k_B T) + CT^n + ATH^m + \frac{B_1}{1+H^2B_2}, \qquad (3)$$

where τ_0 is the preexponential factor in the Arrhenius law, k_B is the Boltzmann constant, C, n, A, B_1 and B_2 are constants. For Kramers ions, the n parameter should be equal to 9 (for Kramers ion with isolated doublets)[20] while m should be equal to 4 (in the case of Co^{II}).[29] However, the n value can be in the range between 1 and 6, when the acoustic and optical phonons are taken into consideration.[33] The QTM process is the main reason why the relaxation processes for compounds having properties of single spins are usually not visible without an applied DC magnetic field.[21]

Assuming that this energy gap does not depend on the magnetic dilution, U_{eff} should be the same for all the synthesized compounds regardless of the dilution. For Co^{II} in tetrahedral com-

plexes, the energy gap can take values from a very wide range, depending on the ligands incorporated in the structure.[27] If the δ value is very high, the Orbach process is very unlikely to occur and the other processes dominate.

We report the preparation and structural and magnetic investigations of $CoBr_2(pyridine)_2$ (**1-Co**) and its diluted analogs $Co_xZn_{1-x}Br_2(pyridine)_2$ ($\mathbf{Co}_x\mathbf{Zn}_{1-x}$) with different Co concentrations, x. The choice of Zn as the diamagnetic equivalent to Co was based on its similar mass and ionic radius. For all the compounds, we determined quantitative changes of the contribution of the QTM/direct processes to the relaxation time. The energy barrier of the Orbach process was determined using three different methods, all of which gave reasonable results. We present that in these compounds the rhombocity is negligible and the energy barrier depends on the D parameter only, which indicates a purely axial symmetry. We also estimated the level of the dilution needed to dispose of the dipolar interaction between magnetic centers enough to be considered negligible, and therefore, the contribution from QTM/direct process.

2 Experimental

2.1 Materials

All reagents were purchased from Sigma Aldrich or Alfa Aesar and used without further purification. Anhydrous cobalt(II) bromide was handled in an inert atmosphere due to its extreme sensitivity to humidity. *Caution! Cobalt(II) bromide is toxic and should be handled with care.*

2.2 Syntheses of $CoBr_2(pyridine)_2$ (1-Co) and $ZnBr_2(pyridine)_2$ (0-Co)

The synthesis of **1-Co** was performed as described in our previus work[15] and the synthesis of **0-Co** was done following a published procedure.[34]

2.3 Syntheses of $Co_xZn_{1-x}Br_2(pyridine)_2$ ($\mathbf{Co}_x\mathbf{Zn}_{1-x}$)

The compound **1-Co** was magnetically diluted with diamagnetic Zn^{II} ions. 5 compounds were sythetised using the following Co salt molar fractions: $x' = 0.1, 0.3, 0.5, 0.7, 0.9$.

x' mmol anhydrous $CoBr_2$ was dissolved in ethanol ($5x'$ ml), $1-x'$ mmol anhydrous $ZnBr_2$ was dissolved in ethanol ($5(1-x')$ ml) and then these solutions were combined together under vigorous stirring. Blue solutions were obtained, to which 2 mmol of pyridine were added. Blue crystals were formed after a few minutes. The average yields were similar in all the cases and stayed around 80%.

2.4 Structural analysis of 1-Co $\mathbf{Co}_x\mathbf{Zn}_{1-x}$ and 0-Co

Powder X-ray diffraction patterns of the polycrystalline samples of pure compounds (**1-Co** and **0-Co**) and solid-solutions ($\mathbf{Co}_x\mathbf{Zn}_{1-x}$) were collected on a Rigaku MiniFlex equipped with Cu-Kα radiation (λ = 1.5418 Å).

2.5 Spectroscopies

Elemental analysis and ICP+MS: Elemental analyses were performed by the standard microanalysis on Elementar Analysensysteme GmbH: vario MICRO cube, while ICP+MS was done by means of Agilent 7700 inductively coupled plasma mass spectrometer (ICP+MS).

Fourier-Transform Infrared (FTIR) spectroscopy: Infrared absorption spectra were recorded with a JASCO IRT-3100 FT-IR microscope for samples dispersed in KBr and compressed in the form of pellets.

Solid state UV-Vis-NIR diffuse-reflectance spectroscopy: Solid state UV-Vis-NIR diffuse-reflectance spectra at room temperature have been recorded for samples spread on the surface of cellulose paper with a JASCO V-670 UV-Vis spectrophotometer equipped with a ISN-723 integrating sphere accessory and converted with the Kubelka-Munk function.

2.6 Magnetic measurements

Polycrystalline samples of **1-Co** and $\mathbf{Co}_x\mathbf{Zn}_{1-x}$ were packed into gelatin capsules, a few drops of nujol were added to assure that the crystals will not rotate in the magnetic field. The gelatin capsule was positioned in a plastic straw of 5 mm diameter. All magnetic measurements were performed using a Quantum Design Magnetic Properties Measurement System 5 XL. All of the DC measurement results were corrected for the diamagnetic contributions of gelatin capsule, nujol and constituent atoms.[35] The static magnetic susceptibility for **1-Co** and $\mathbf{Co}_x\mathbf{Zn}_{1-x}$ was fitted with the analytical formula obtained by applying generalized van Vleck formalism to determine full magnetic susceptibility tensor for a system with S = 3/2 for powder samples (Eq. S1).[36] Four parameters were derived: D, E, g_{xy} and g_z.

All of the AC magnetic measurements were performed at H_{AC} = 3 Oe and H_{DC} = 2.5 kOe. The frequency dependences of AC magnetic susceptibility of **1-Co** and $\mathbf{Co}_x\mathbf{Zn}_{1-x}$ were measured at the temperatures from the range 1.8 – 3.24 K.To analyse the data, single-mode Cole-Cole model:

$$\chi_{AC} = \chi_0 + \frac{\chi_1}{1+(i\omega\tau_1)^{1-\alpha_1}}, \tag{4}$$

or double-mode Cole-Cole model:

$$\chi_{AC} = \chi_0 + \frac{\chi_1}{1+(i\omega\tau_1)^{1-\alpha_1}} + \frac{\chi_2}{1+(i\omega\tau_2)^{1-\alpha_2}}, \tag{5}$$

were used, where χ_0 is the adiabatic limit of magnetic susceptibility, χ_1 and χ_2 are the amplitudes of the processes, τ is a relaxation time and α parameter describes the dispersion of relaxation times.[37]

The obtained values of relaxation times τ were plotted as their logarithms vs. inverse temperature for **1-Co** and $\mathbf{Co}_x\mathbf{Zn}_{1-x}$. Firstly, the Arrhenius law was fitted to the linear, high temperature regimes of the points' courses for all compounds, and the values of τ_0 and U_{eff} were determined. Secondly, to all of the points, Eq. 3 was fitted. The pathways of relaxation times were found and the parameters describing them were determined quantitatively.

All the data obtained from magnetic measurements were pro-

cessed using the OriginPro 2018 software.

3 Results and discussion

3.1 Syntheses and structures

Syntheses of 1-Co Co_xZn_{1-x} and 0-Co: Color intensity of the resulting products depended on the x' value, which suggests that the obtained crystals are indeed solid solutions. The higher the x', the more intense the color of the crystals, as presented in Fig. 1. The crystals of **0-Co** (not included in Fig. 1.) are white.

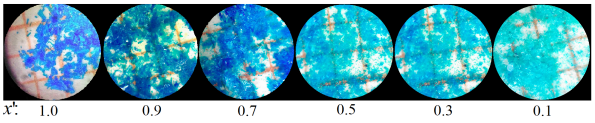

Fig. 1 The photos of **1-Co** and **Co_xZn_{1-x}** crystals. Grid size = 1 mm.

Structures: Single crystal X-ray structures of pure phases of $Co(py)_2Br_2$, **1-Co** ($x = 1$) and $Zn(py)_2Br_2$, **0-Co** ($x = 0$) have recently been reported (Fig. S1).[15,34] Both materials crystallized in the monoclinic space group $P2_1/c$ with almost identical unit cell parameters: $a = 8.6842(10)$ Å, $b = 18.1757(18)$ Å, $c = 8.5209(8)$ Å, $\beta = 100.878(7)^\circ$ and $V = 1320.78$ Å^3 for **1-Co**; and $a = 8.7388(5)$ Å, $b = 17.9730(10)$ Å, $c = 8.5452(5)$ Å, $\beta = 100.024(6)^\circ$ and $V = 1321.64$ Å^3 for **0-Co**. Structural units of **1-Co** and **0-Co** consist of distorted tetragonal cobalt(II) and zinc(II) complexes, respectively, which central metal ions are coordinated by two nitrogen atoms of two symmetry independent pyridine ligands and two bromide anions.

Average Co–N and Co–Br distances for **1-Co** are equal to 2.023 and 2.370 Å, respectively, while **0-Co** shows very similar bond lengths equal to 2.051 and 2.352 Å, respectively. Moreover, N–Co–N, average N–Co–Br, and Br–Co–Br angles for **1-Co** adopt values of 108.4°, 107.4° and 118.4° in series. In the case of **1-Co** the N–Co–N angle is slightly smaller with a value of 105.1°, average N–Co–Br angle remains unchanged (107.5°), and Br–Co–Br angle is slightly larger with the value of 120.7°. It is noteworthy that despite the differences in the mutual orientation of the aromatic ring planes, both systems generate identical packing inside the unit cells.

Measured powder diffractograms and simulated ones ($x = 1$ and 0) for single crystals of **1-Co** and **0-Co** are almost identical (Figure 2). These confirm the isostructural character and phase purity of synthesized materials. Differences in the intensities of diffraction peaks can be assigned to the effect of preferred orientation along the a-crystallographic direction. Furthermore, an in-depth analysis of diffraction data for peaks around 16.8°, 22.3° and 31.3° two theta angle for compounds with diverse x values showed that crystal structures evolve gradually with change of compositions and there is in no case when two distinguishable phases **1-Co** and **0-Co** exist independently (Figures S2b-d). All of these results confirm the successful obtaining of a perfect solid-solution. Additionally, systematic analysis of the linear shift of peak positions around 31.3° 2-θ (Figure S2d) can be used for a rough determination of the Co:Zn ratio in the materials (Table S1) which match the results of the ICP+MS analysis (see the next section).

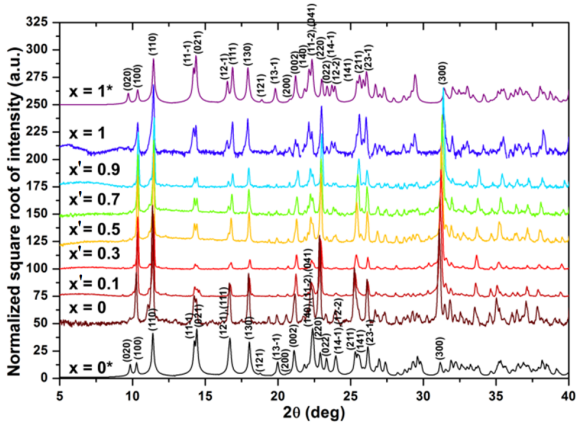

Fig. 2 Measured powder X-ray diffractograms for solid-solutions and simulated ones (*) for single crystal structures of **1-Co**, **Co_xZn_{1-x}** and **0-Co**. Initial concentrations, x', are indicated in the figure.

3.2 Determination of the Co concentration

The values of x' used in the syntheses of **Co_xZn_{1-x}** were: 0.9, 0.7, 0.5, 0.3, 0.1. The real concentrations of Co, x, determined from the low-temperature field dependence of magnetization (Fig. S5), ICP+MS and PXRD are presented in Table 1. Results of ICP+MS and PXRD analyses are consistent and they lead to a general conclusion that the cobalt to zinc ratios used in syntheses are well reflected in the final products (Table S2). Furthermore, these values are close to the ratio determined from magnetic measurements.

Table 1 The content of Co in **Co_xZn_{1-x}** determined from magnetic measurements, ICP+MS and PXRD

x'	x from magnetiztion curve	x from ICP+MS	x from PXRD
0.9	0.78	0.91	0.9
0.7	0.52	0.67	0.6
0.5	0.34	0.43	0.3
0.3	0.23	0.24	0.24
0.1	0.049	0.06	0.06

As can be seen, the concentrations determined by ICP+MS and PXRD differ by around 10% from the concentrations determined from the field dependence of the magnetization, they also are in better agreement with x'. This case is different from the case of the compound formed by $CoBr_2$ with macormolecules[15], where values from magnetic measurements and from ICP+MS were in agreement. This is probably due to the stiffness of crystals compared to soft matter. In this case, we decided to use the values determined by ICP+MS in all the other analyses, as it is the most precise method to determine atomic concentrations.

3.3 Spectroscopic measurements

Additionally, to check the homogeneity of the samples, FTIR spectroscopy was performed for all the compounds. All spectra are almost identical with slight shifts of peaks positions for solid-solutions due to gradual evolution of composition and there is no case when two distinguishable phases **1-Co** and **0-Co** exist independently (Figure S3). These observations confirm the successful obtaining of a perfect solid-solution. It is noteworthy to mention that this gradual change also leads to the generation of

an isosbestic point at around 642 cm^{-1} (see Figure 3).

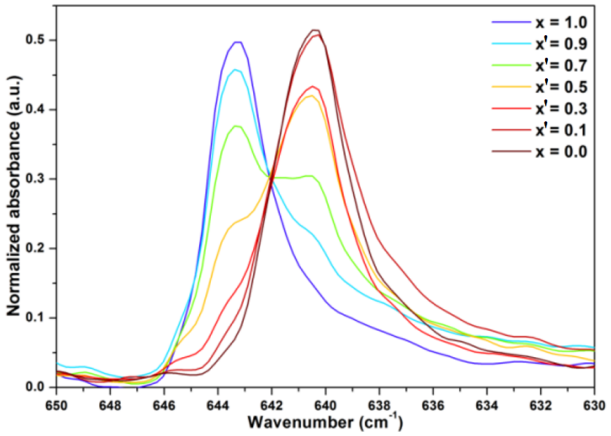

Fig. 3 FTIR measurements results for pure compounds (**1-Co** and **0-Co**) and solid-solutions ($\mathbf{Co}_x\mathbf{Zn}_{1-x}$). Clearly visible isosbestic point at around 642 cm^{-1}.

We also performed solid state UV-Vis-NIR diffuse-reflectance spectroscopy for all the compounds. Analysis of normalized spectra (Figure S4) revealed several characteristic features such as: i) all materials containing cobalt(II) show three similar absorption regions: below 400 nm (below 25000 cm^{-1}), 500 - 700 nm (20000 - 14300 cm^{-1}) and 900 - 2000 nm (9900 - 5000 cm^{-1}), which can be deconvoluted in five, five and four Gaussian components, respectively (Table S3); ii) intensities of the most of peaks decrease with diminishing Co(II) concentration, however, there is no simple equation which can correlate the observed changes in spectra with Co:Zn ratio; iii) spectrum of the pure zinc(II) complex (**0-Co**) is the simplest one due to the presence of absorption bands below 300 nm originating from pyridine, which can also be deconvoluted into five Gaussian components. More details can be found in ESI.

3.4 Magnetic properties

The temperatre dependence of DC magnetic susceptibility measured at 1 kOe for **1-Co** and $\mathbf{Co}_x\mathbf{Zn}_{1-x}$ is presented in Fig. 4. as the χT product. The value of χT at 240 K for **1-Co** is 2.38 $cm^3{\cdot}K{\cdot}mol^{-1}$, which is slightly larger than the value expected for a compound with the magnetic centers characterized by an isotropic spin $S = 3/2$ - 1.875 $cm^3{\cdot}K{\cdot}mol^{-1}$. The values for $\mathbf{Co}_x\mathbf{Zn}_{1-x}$ with x values equal 0.91, 0.67, 0.43, 0.24, 0.06 are 1.84, 1.27, 0.85, 0.57, 0.13 $cm^3{\cdot}K{\cdot}mol^{-1}$, respectively.

For all the compounds in the χT product, no peak is visible in the whole range of temperature, which proves that there is no long-range magnetic ordering. The fluctuations of the populations of the M_S levels for the ground state of the spin are the reason for the decrease of χT below 40 K for all the compounds. It is a characteristic feature of a system of noninteracting anisotropic spins.

The fitting of χT vs. T dependences with the formula proposed by R. Pełka[36] (Equation S1), revealed that the E parameter ($\sim 10^{-5}$ K) is around 6 orders of magnitude lower than the $|D|$ parameter ($\sim$10 K), and for that reason, it was neglected for all the compounds. That indicates that the anisotropy is of purely axial character. The results are presented in Table 2. together with the g factors and the estimated energy gaps, δ, according to Eq. 2.

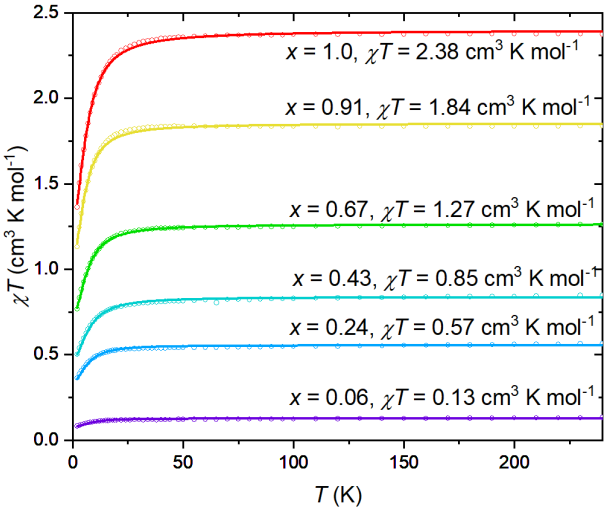

Fig. 4 The temperature dependence of magnetic susceptibility χ measured at 1 kOe presented as the χT product for **1-Co** and $\mathbf{Co}_x\mathbf{Zn}_{1-x}$. The solid lines are the fits of the Eq. S1 (see text).

Table 2 The values of axial zero-field splitting parameter D, the energy gap between ground and first excited state in Co^{II}, δ, g_{xy} and g_z.

x	D (K)	$\delta = 2\|D\|$ (K)	g_{xy}	g_z
1.0	-9.52(23)	19.04(46)	2.368(6)	2.03(2)
0.91	-8.49(37)	16.98(74)	2.152 (9)	1.94(2)
0.67	-10.14(20)	20.28(40)	2.064 (4)	1.883(8)
0.43	-11.49(55)	23.0(1.1)	2.10 (1)	1.90(2)
0.24	-10.62(87)	21.2(1.7)	2.25(2)	2.16(4)
0.06	-13.5(2.1)	27.0(4.2)	2.14(3)	2.08(6)

The D parameter should be the same for all the compounds because the energy level scheme of Co^{II} cannot be affected by the magnetic dilution (the distribution of the dipolar field cannot influence the energy level scheme). The obtained values are all around -10 K, with a slight deviation for $\mathbf{Co}_x\mathbf{Zn}_{1-x}$ with $x = 0.06$, for which, however, the fit is the least accurate. The values of the g-factors are around 2.0 for g_z and more than 2.1 for g_{xy} for all of the compounds, thus, non-neglegible anisotropy of the g factor is confirmed. The estimated energy barrier of the relaxation process should then equate around 20 K. The D parameter is negative in every case, which confirms that the lowest lying states are indeed those with $M_S = \pm 3/2$.

To obtain the energy barrier of the relaxation process in a different way, the AC magnetic measurements were performed. The magnetic relaxation process is not visible at $H_{DC} = 0$ for **1-Co** and $\mathbf{Co}_x\mathbf{Zn}_{1-x}$, which is a very common situation for SIMs, because of very fast quantum tunneling of magnetization.[29] In a sufficiently strong magnetic field, the relaxation process is visible, which was confirmed by the AC magnetic susceptibility measured at 2.5 K in fields from the range 0–4 kOe and at four different AC field frequencies (1, 10, 100 and 1000 Hz) for **1-Co** (Fig. S6). The field of 2.5 kOe was chosen as optimal for further measurements, as there the χ'' value reaches a maximum at 1000 Hz. Due to the

competition between quantum tunneling of magnetization and direct processes (see below), at very low fields and at very high fields the relaxation processes become too fast to observe them experimentally. Diluted compounds behave similarly, thus, the further AC magnetic measurements for **1-Co** and $\mathbf{Co}_x\mathbf{Zn}_{1-x}$ were performed at H_{DC} = 2.5 kOe.

The temperature dependences of AC magnetic susceptibility of **1-Co** and $\mathbf{Co}_x\mathbf{Zn}_{1-x}$ were measured at four different frequencies (Fig. S7). The blocking temperature is not affected by the dilution and is around 3 K in all cases.

Frequency dependences of AC magnetic susceptibility measured at temperatures from the range 1.8 - 3.24 K in H_{DC} = 2.5 kOe are presented for all the compounds in Fig. 5. as Argand plots. For **1-Co** and $\mathbf{Co}_x\mathbf{Zn}_{1-x}$ with x = 0.91, 0.67, the double-mode Cole-Cole model was used to analyse the data due to the clearly visible two different processes of relaxation. The faster relaxation process with a higher χ'' amplitude is hereby called the *1. relaxation step* and the slower process with lower amplitude is called the *2. relaxation step*. For $\mathbf{Co}_x\mathbf{Zn}_{1-x}$ with x = 0.43, 0.24, 0.06, the single-mode Cole-Cole model was used to analyse the data. The parameters obtained from fitting the Cole-Cole model are presented in Tables S4-S9. The χ_0 parameter, the adiabatic limit of the magnetic susceptibility corresponds to the spins for which the spin-lattice relaxation does not occur, but spin-spin relaxation is possible.[38,39] The χ_0 values decrease with the dilution and no temperature dependence is observed.

For the *1. relaxation step* the maxima of χ'' are shifted to the lower frequencies with increasing dilution (Fig. S9.), which means longer times of relaxation. The *2. relaxation step* decreases and eventually vanishes with increasing dilution, for $\mathbf{Co}_x\mathbf{Zn}_{1-x}$ with x = 0.43, 0.24, 0.06 being no longer possible to analyse. The obtained values of relaxation times for the *1. relaxation step*, τ, were plotted as their logarithms vs. inverse temperature (Fig.6).

The simplified analysis of relaxation times for the *1. relaxation step* was conducted for all of the compounds, where only the contribution from the Orbach process was taken into consideration – many researchers limit their analysis to only this procedure. Fitting of the Arrhenius expression to the high-temperature, linear part of $\ln\tau$ vs. $1/T$ dependences for **1-Co** and $\mathbf{Co}_x\mathbf{Zn}_{1-x}$ (Fig. 6, top) enabled the determination of the effective energy barriers of the Orbach process, U_{eff}/k_B. The obtained values together with preexponential factors are presented in Table 3. The energy barriers are in the range from 14 to 27 K, which is loosely consistent with the assumption that the energy gap between the ground and the first excited state cannot be affected by the dilution. However, the fitting of Arrhenius law only does not describe the whole temperature range of the relaxation times because of the other processes that shorten τ at lower temperatures. This is significant in our case as the largest differences between diluted compounds arise at low temperatures.

A more accurate analysis was performed, in which the whole Eq. 3. was considered for fitting to the $\ln(\tau)$ vs. $1/T$ dependences in the whole temperature range. As fitting the whole said equation in an unaltered form is impossible due to mutual dependence between the parameters, a reasonable simplification is in order. The values of the relaxation time for **1-Co**, which reach a plateau

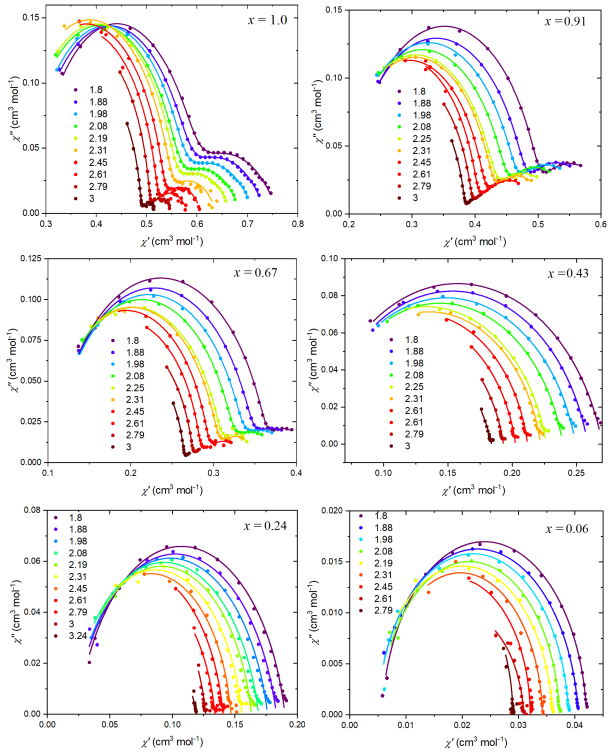

Fig. 5 Argand plots of AC magnetic susceptibility of **1-Co** and $\mathbf{Co}_x\mathbf{Zn}_{1-x}$ measured for all 6 compounds at H_{DC} = 2.5 kOe and H_{AC} = 3 Oe at temperatures from the range 1.8–3.24 K.

Table 3 The values of effective enrgy barrier U_{eff}/k_B and preexponential factor τ_0 for **1-Co** and $\mathbf{Co}_x\mathbf{Zn}_{1-x}$ determined assuming the Orbach process as the pathway of relaxation in high-temperature regime.

x	U_{eff}/k_B (K)	τ_0 (s)
1.0	13.8(8)	$1.7(6)\cdot10^{-9}$
0.91	14.8(6)	$1.7(6)\cdot10^{-9}$
0.67	17.3(7)	$4.5(2.2)\cdot10^{-9}$
0.43	23.8(1.3)	$1.0(3)\cdot10^{-7}$
0.24	27.2(8)	$4.3(1.3)\cdot10^{-7}$
0.06	26.1(5)	$2.7(6)\cdot10^{-7}$

in the low-temperature regime, suggest that the relaxation can be proceeded by QTM, non-negligible next to the Orbach process.

Bearing in mind that the AC magnetic susceptibility exhibits a maximum in the DC field dependence, we assume that the direct and QTM processes should contribute to the relaxation. The equation describing QTM and direct processes contributions in the simplest form, which does not include the field dependence, is:

$$\tau^{-1}_{QTM+direct} = B' + A'T = B'', \quad (6)$$

where B' describes QTM ($B_1/(1+B_2)$ in Eq. 3.) and A' describes the direct process (AH^4 in Eq.3.). As the accessible temperature range is narrow, during the fitting procedure of the simplified model, these two processes are almost indistinguishable. For that reason, QTM or direct process were fitted as one constant, B''. The best fits (Fig. 6, bottom) were obtained when the Raman process was excluded. The attempt to include the Raman process as well delivered unreasonable C parameters. The T^9 dependence of the Raman process would cause a much stronger

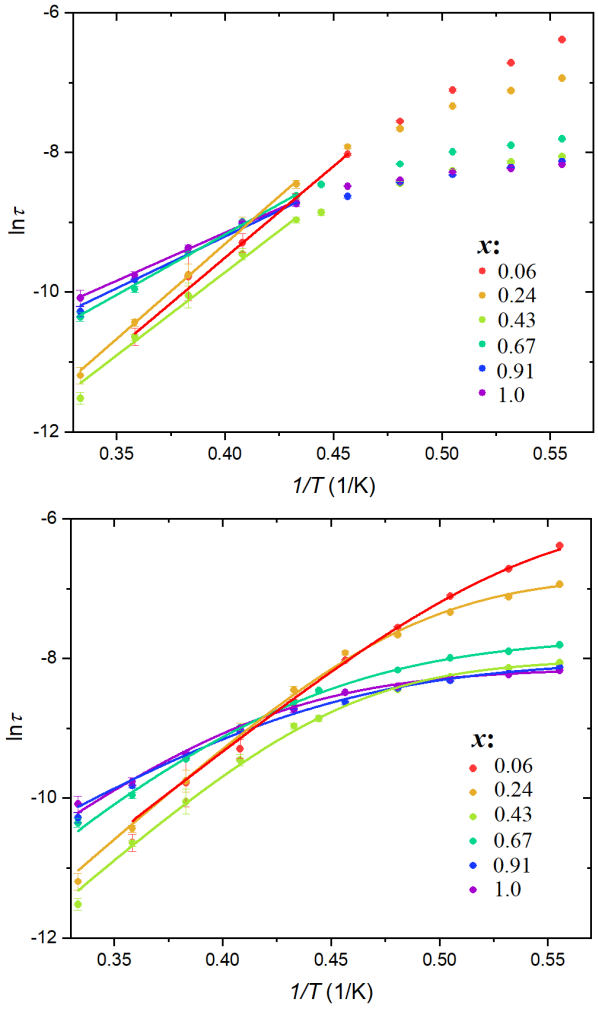

Fig. 6 Arrhenius plot for **1-Co** and $\mathbf{Co}_x\mathbf{Zn}_{1-x}$ for dependences measured at H_{DC} = 2.5 kOe. Top: Solid lines are fits of the Arrhenius expression. Bottom: Solid lines are fits of Eq. 3. to the all points of lnτ vs. *1/T* dependance.

change within the studied temperature range, which is not the case here. Furthermore, taking into account the already deduced competition between field-dependent QTM and direct processes causing the maximum in the χ'' AC susceptibility vs. DC field dependence, which would not be explained by the Raman process, we decided to exclude the latter altogether. The obtained values are presented in Table 4.

The QTM and/or direct process is suppressed with the dilution and the relaxation times become longer. What must be underlined is the fact that the values of the energy barriers are close to the values of δ obtained from the analysis of the DC magnetic susceptibility vs. T dependence. The QTM and/or direct process will become negligible next to the Orbach process below 5% of Co content.

The analysis of magnetic relaxation processes - 2. relaxation step

The *2. relaxation step* is vanishing with the dilution. The Arrhenius plots for this relaxation process are presented in Fig. S8.

Table 4 The values of B'' and Δ/k_B obtained from fitting Eq. 3 without Raman process for **1-Co** and $\mathbf{Co}_x\mathbf{Zn}_{1-x}$.

x	B'' (s^{-1})	Δ/k_B (K)
1.0	3448(71)	22.5 (1.6)
0.91	3060(120)	18.4(1.7)
0.67	2170(140)	20.9(3.2)
0.43	3025(75)	27.0(1.0)
0.24	911(42)	27.1(1.2)
0.06	377(49)	24.3(1.4)

The relaxation times have quite large errors which is the result of the small amplitude of this relaxation process. For the most diluted compounds (x = 0.43, 0.24, 0.06) the *2. relaxation step* is no longer visible in AC magnetic susceptibility measurements. The presence of the second relaxation step is the result of strong dipolar interactions and collective nuclear magnetic field.[26] That indicates that the same mechanism is responsible for the suppression of direct or QTM processes and the existence of multiple relaxation processes - which is consistent with the fact that the constant B'' decreases with the dilution, the *2. relaxation step* also vanishes.

For a single Kramers ion, two relaxation steps can appear when the QTM and direct processes have their contribution to the χ'' of the same order of magnitude.[26] Then, two frequency domains are created - the first one mainly responsible for the QTM and the second one mainly for the direct process. These frequency domains can overlap, so the maxima in χ'' cannot be assigned unequivocally to the single process. When the contribution of one process begins to dominate, the maxima blend together. In the case of magnetic dilution, the average dipolar field decreases, so the relative contribution to χ'' from the direct process should decrease and from QTM increase, which effectively means that the ratio of amplitudes of the *1.* and *2. relaxation steps* (χ''_1/χ''_2) should increase. This is qualitatively visible in Fig. 3. Such a quantitative analysis was performed for a seven-coordinate Co(II) complex[31] on the basis of which, the second relaxation process was determined as of intermolecular origin. In our work we draw a consistent conlusion that the creation of the two frequency domains is of intermolecular origin.

On that basis, we can only suspect that for the *1. relaxation* step the QTM process is responsible, and for the *2. relaxation step* - the direct process. However, the two considered processes, QTM and the direct process are indistinguishable in the given temperature range. For the most diluted samples, (x = 0.43, 0.24 and 0.06), the maxima blend together, which indicates the creation of the only one frequency domain (in the accessible frequencies range).

4 Conclusions

We presented thorough investigations of the properties a mononuclear compound based on Co^{II} ion exhibiting Single Ion Magnet properties, $CoBr_2(pyridine)_2$ (**1-Co**). To take a deeper insight into the relaxation process, we successfully synthesised 5 diluted analogs of **1-Co**, $Co_xZn_{1-x}Br_2(pyridine)_2$, with different x value, to check its influence on the magnetic relaxation and estimate the value of the energy barrier. Using X-Ray diffraction and spectroscopies we confirmed that the series we obtained is a

perfect solid solution.

The energy barrier was estimated using three different types of analysis. From static magnetic susceptibility for all the compounds we determined zero-field splitting parameters, D and E (the latter was found close to zero). Using these values, we calculated the energy gap between the two lowest lying Kramers doublets, δ, and proved that for this compound, the rhombocity is indeed negligible, which confirms the axial nature of anisotropy. The sign of the D parameter is negative which means that the lowest lying Kramers doublet are levels with $M_S = \pm 3/2$.

The δ parameter should be equal to the energy barrier of the Orbach relaxation process which was checked by analysing the dynamic magnetic susceptibility. All the measurements were performed at 2.5 kOe, as at around that field, the field dependence of χ'' displays a maximum. Taking into consideration the whole accessible temperature regime to determine the energy barrier, not only the linear, high-temperature part, enabled us to determine the energy barrier, Δ/k_B, which is in better agreement with δ than the value of the effective energy barrier determined using the simplified analysis with the Orbach process alone. In this detailed analysis, we assume that the contribution to the relaxation time of the *1. step* most probably arises from QTM/direct and Orbach processes. In the field dependence of χ_{AC} a weak maximum is visible, which indicates the presence of the direct process. This process is visible as the second maximum in χ" vs. χ' dependence (also χ" vs. f, Fig. S9) for samples with $x = 1.0$, 0.91, 0.67. For the other samples, the maxima blend together as a result of significantly reduced dipolar interactions between magnetic ions, which indicate the disappearance of the maximum of the low-frequency domain. The maximum of the high-frequency domain (short times) remains.

Our research is a thorough investigation of the influence of magnetic dilution on the relaxation processes in SIMs in the whole range of stoichiometric ratios of the magnetic to diamagnetic ions. We confirm that in this case the contribution of the QTM and direct processes vanishes monotonously with increasing dilution, and gather a detailed way to analyse both the DC and AC magnetic properties of such compounds. We confirm that diluting crystalline SIM compounds with diamagnetic species is an effective way to lower the probability of the low-temperature processes that shorten the relaxation times down to the point of negligibility. We believe that this research will be useful for all the scientists working on synthesizing new SIM compounds to estimate the optimal dilution of their samples, and will be useful regarding the future applications of such materials.

Conflicts of interest

The authors declare no competing financial interests.

Acknowledgements

This research was financed by the Polish National Science Centre within the SONATA Project UMO–2015/19/D/ST5/01936. This work was supported by the Japan Society for the Promotion of Science within the Grant–in–Aid for Specially Promoted Research (15H05697) and the Grants–in–Aid for Scientific Research on Innovative Areas Soft Crystals (area No. 2903, 17H06367). This work was partially supported by MEXT Quantum Leap Flagship Program (MEXT Q–LEAP) Grant Number JPMXS0118068681. We also acknowledge The University of Tokyo Cryogenic Research Center and Center for Nanolithography & Analysis, which are supported by MEXT.

Notes and references

1 D. Gatteschi, R. Sessoli and J. Villain, *Molecular nanomagnets*, Oxford University Press, New York, 1st edn, 2006.
2 J. Ferrando-Soria, J. Vallejo, M. Castellano, J. Martínez-Lillo, E. Pardo, J. Cano, I. Castro, F. Lloret, R. Ruiz-García and M. Julve, *Coord. Chem. Rev.*, 2017, **339**, 17–103.
3 M. Cavallini, J. Gomez-Segura, D. Ruiz-Molina, M. Massi, C. Albonetti, C. Rovira, J. Veciana and F. Biscarini, *Angew. Chem. Int. Ed.*, 2005, **44**, 888–892.
4 G. A. Craig and M. Murrie, *Chem. Soc. Rev.*, 2015, **44**, 2135–2147.
5 F.-S. Guo, B. M. Day, Y.-C. Chen, M.-L. Tong, A. Mansikkamaki and R. A. Layfield, *Science*, 2018, **362**, 1400–1403.
6 D. N. Woodruff, R. E. P. Winpenny and R. A. Layfield, *Chem. Rev.*, 2013, **113**, 5110–5148.
7 P. Zhang, Y.-N. Guo and J. Tang, *Coord. Chem. Rev.*, 2013, **257**, 1728–1763.
8 A. Dey, P. Kalita and V. Chandrasekhar, *ACS Omega*, 2018, **3**, 9462–9475.
9 Y.-S. Meng, L. Xu, J. Xiong, Q. Yuan, T. Liu, B. Wang and S. Gao, *Angew. Chem.*, 2018, **57**, 4673–4676.
10 A. B. Canaj, M. Kumar, C. Wilson, G. Rajaraman and M. Murrie, *Chem. Commun.*, 2018, **54**, 8273–8276.
11 M. Feng and M. Tong, *Chem. Eur. J.*, 2018, **24**, 7574–7594.
12 C. A. P. Goodwin, F. Ortu, D. Reta, N. F. Chilton and D. P. Mills, *Nature*, 2017, **548**, 439–442.
13 O. Kahn, *Molecular magnetism*, VCH, New York, 1st edn, 1993.
14 J. M. Frost, K. L. M. Harriman and M. Murugesu, *Chem. Sci.*, 2016, **7**, 2470–2491.
15 A. M. Majcher, P. Dąbczyński, M. M. Marzec, M. Ceglarska, J. Rysz, A. Bernasik, S. Ohkoshi and O. Stefańczyk, *Chem. Sci.*, 2018, **9**, 7277–7286.
16 S. Chorazy, J. J. Stanek, W. Nogaś, A. M. Majcher, M. Rams, M. Kozieł, E. Juszyńska-Gałązka, K. Nakabayashi, S. Ohkoshi, B. Sieklucka and R. Podgajny, *J. Am. Chem. Soc.*, 2016, **138**, 1635–1646.
17 H. A. Kramers, *Proc. K. Akad. Wet.*, 1930, **33**, 959–972.
18 S. Gomez-Coca, A. Urtizberea, E. Cremades, P. J. Alonso, A. Camon, E. Ruiz and F. Luis, *Nat. Commun.*, 2014, **5**, 1–8.
19 Y.-Y. Zhu, F. Liu, J.-J. Liu, Y.-S. Meng, S.-D. Jiang, A.-L. Barra, W. Wernsdorfer and S. Gao, *Inorg. Chem.*, 2017, **56**, 697–700.
20 R. L. Carlin, *Magnetochemistry*, Springer-Verlag, Berlin, Heidelberg, New York, Tokyo, 1st edn, 1986.
21 J. M. Zadrozny, M. Atanasov, A. M. Bryan, C.-Y. Lin, B. D. Rekken, P. P. Power, F. Neese and J. R. Long, *Chem. Sci.*, 2013, **4**, 125–138.

22 Y. Rechkemmer, F. D. Breitgoff, M. van der Meer, M. Atanasov, M. Hakl, M. Orlita, P. Neugebauer, F. Neese, B. Sarkar and J. van Slageren, *Nat. Commun.*, 2016, **7**, 10467.

23 R. Boca, C. Rajnak, J. Moncol, J. Titis and D. Valigura, *Inorg. Chem.*, 2018, **57**, 14314–14321.

24 J. Ruiz, A. J. Mota, A. Rodriguez-Dieguez, S. Titos, J. M. Herrera, E. Ruiz, E. Cremades, J. P. Costesc and E. Colacio, *Chem. Commun.*, 2012, **48**, 7916–7918.

25 S. Sottini, G. Poneti, S. Ciattini, N. Levesanos, E. Ferentinos, J. Krzystek, L. Sorace and P. Kyritsis, *Inorg. Chem.*, 2016, **55**, 9537–9548.

26 L. T. A. Ho and L. F. Chibotaru, *Phys. Rev. B*, 2018, **98**, 174418.

27 J. M. Zadrozny, J. Telser and J. R. Long, *Polyhedron*, 2013, **64**, 209–217.

28 L. Chen, S.-Y. Chen, Y.-C. Sun, Y.-M. Guo, L. Yu, X.-T. Chen, Z. Wang, Z. W. Ouyang, Y. Songa and Z.-L. Xue, *Dalton Trans.*, 2015, **44**, 11482–11490.

29 M. A. Palacios, J. Nehrkorn, E. A. Suturina, E. Ruiz, S. Gomez-Coca, K. Holldack, A. Schnegg, J. Krzystek, J. M. Moreno and E. Colacio, *Chem. Eur. J.*, 2017, **23**, 11649–11661.

30 K. R. Meihaus, J. D. Rinehart and J. R. Long, *Inorg. Chem.*, 2011, **50**, 8484–8489.

31 F. Habib, I. Korobkova and M. Murugesu, *Dalton Trans.*, 2015, **44**, 6368–6373.

32 A. Abragam and B. Bleaney, *Electron paramagnetic resonance of transition ions*, Clarendon Press - Oxford, London, 1st edn, 1970.

33 K. N. Shrivastava, *Phys. Stat. Sol. B*, 1983, **117**, 437–458.

34 H. Ishihara, M. Nakashima, H. Nakashima, R. Tateno, Y. Shibamura, T. Makino, A. Kikuchiu, D. Kii, K. Horiuchi, I. Svoboda, H. Fuess and H. Terao, *Z. Naturforsch., B: Chem. Sci.*, 2011, **66**, 27.

35 G. A. Bain and J. F. Berry, *J. Chem. Educ.*, 2008, **85**, 532–536.

36 R. Pełka, *Acta Phys. Pol. A*, 2011, **119**, 428–436.

37 K. S. Cole and R. H. Cole, *J. Chem. Phys.*, 1941, **9**, 341–351.

38 A. H. Morrish, *The Physical Principles of Magnetism*, Wiley-VCH, New York, 1st edn, 2001.

39 M. Bałanda, *Acta Phys. Pol. A*, 2013, **124**, 964.

Influence of magnetic dilution on relaxation processes in a solid solution comprising tetrahedral Co/Zn^{II} complexes

Magdalena Ceglarska[a], Olaf Stefańczyk[b], Shin-ichi Ohkoshi[b], and Anna M. Majcher-Fitas[*a]

[a]Faculty of Physics, Astronomy and Applied Computer Science, Jagiellonian University, Łojasiewicza 11, 30–348 Krakow, Poland

[b]Department of Chemistry, School of Science, The University of Tokyo, 7-3-1 Hongo, Bunkyo-ku, Tokyo 113-0033, Japan

Table of Contents

Dilution with diamagnetic species in a SIM solid solution leads to increase in relaxation times at low temperatures and monotonously reduces the probability of quantum tunneling of magnetization and direct process.